Matrix: Jurnal Manajemen Teknologi dan Informatika
Volume 16 Issue 1 Year 2026 Pages 29-38
DOI: http://dx.doi.org/10.31940/matrix.v16i1.29-38
URL: http://ojs2.pnb.ac.id/index.php/matrix

Bell's Palsy and stroke face classification using SVM with MediaPipe Face Mesh

Chelsea Effendi [1], Destriana Widyaningrum [2]*

[1,2] *Informatics Study Program, Universitas Bunda Mulia, Indonesia*

*Corresponding Author: *l0894@lecturer.ubm.ac.id*

Abstract: Stroke and Bell's Palsy share similar manifestations of unilateral facial paralysis, often leading to clinical misinterpretation, particularly in acute cases. Although deep learning approaches have demonstrated strong performance in segmenting facial paralysis regions, these methods primarily focus on area localization rather than directly differentiating Stroke and Bell's Palsy, and typically require large-scale datasets and substantial computational resources. To address this gap, this study proposes an explainable and resource-efficient framework for classifying Stroke and Bell's Palsy using asymmetric facial numeric features extracted from static images. Unlike appearance-based deep learning models, the proposed approach transforms facial landmarks detected by MediaPipe Face Mesh into geometric asymmetry features through Min–Max scaling, Euclidean distance, and angle computation. After class balancing via undersampling, classification was performed using an SVM with an RBF kernel. The 70:30 split achieved the most stable performance, with a testing accuracy of 0.8041 and cross-validation accuracy of 0.8072 ± 0.0069, indicating minimal generalization gap. These findings demonstrate that geometric asymmetry features combined with SVM provide a reliable and interpretable alternative for differentiating BP and ST under limited data and computational constraints.

Keywords: Bell's Palsy, facial asymmetry, machine learning, MediaPipe Face Mesh, stroke, Support Vector Machine

History Article: Submitted 23 January 2026 | Revised 13 February 2026 | Accepted 14 February 2026

How to Cite: C. Effendi and D. Widyaningrum, "Bell's Palsy and stroke face classification using SVM with MediaPipe Face Mesh," *Matrix: Jurnal Manajemen Teknologi dan Informatika*, vol. 16, no. 1, pp. 29–38, 2026, doi: 10.31940/matrix.v16i1.29-38.

Introduction

Stroke (ST) is an acute medical condition caused by vascular injury to the central nervous system [1]. In the simplest terms, stroke occurs when the blood supply to the brain is disrupted, causing areas of the brain that lack oxygen and nutrients to die [2]. Thus, if the affected area involves the region of the brain responsible for facial nerves, one of the symptoms is facial paralysis. Its etiology involves a wide range of risk factors, such as hypertension, obesity, high cholesterol, genetic predisposition, and progression from cardiovascular diseases. On the other hand, Bell's Palsy (BP) is a non-progressive acute medical condition characterized by temporary weakness or paralysis of the facial muscles [3]. These similar symptoms led people with acute unilateral upper and lower facial palsy to believe that they had experienced a stroke, when in fact it was benign Bell's palsy [4]. Furthermore, a study on ischemic stroke reported that 24.8% of cases were stroke mimics, of which 5% were mononeuropathies, including BP [5]. So far, the exact etiology of Bell's Palsy remains uncertain. However, several studies suggest that it may be associated with viral infections, trauma, or specific syndromes, with additional contributing factors such as pregnancy, diabetes, and even environmental conditions [3], [6], [7].

Studies on facial asymmetry have been conducted using deep learning models to segment paralyzed areas within a face [2]. These approaches have demonstrated strong performance, particularly when trained on large-scale and diverse datasets. However, achieving such high performance with deep learning models is closely associated with the availability of large-scale and diverse datasets, as well as substantial computational resources. In addition, privacy and ethical issues surrounding facial data make the data-collection process even more challenging. The study in [2] was conducted using 18,840 facial images of Bell's palsy and private dataset

consisting of approximately 1,435 facial images of Stroke patients, which may not be readily accessible for independent replication or comparative evaluation.

In contrast, the publicly available datasets identified for this study are considerably smaller, particularly for Bell's Palsy cases, for which only 10,754 facial images were obtainable. Furthermore, only 2,279 facial images of Stroke cases were available, resulting in a significant class imbalance that may cause classification bias. To address these data constraints, this study applies an undersampling strategy to mitigate class imbalance and adopts Support Vector Machine (SVM), a supervised machine learning algorithm known for its robustness when trained on limited datasets and suitable for resource-limited environments [8], [9]. The proposed framework is designed to classify Bell's Palsy and Stroke based on asymmetric facial numeric features extracted from static facial images using a Support Vector Machine (SVM) classifier.

A previous evaluation also identified SVM as the more accurate model, achieving 96.59% and outperforming XGB and RF while maintaining high precision, recall, F1-score, and Matthews Correlation Coefficient [10]. A comparative study between CNN and SVM showed that CNN achieved higher classification performance, but required significantly greater computational resources and twice the training time [8]. These findings align with the needs of this study, reinforcing SVM as an appropriate baseline for differentiating Bell's Palsy and Stroke.

Rather than directly analyzing facial appearance, this study employs MediaPipe Face Mesh (MFM) as a geometric abstraction tool to convert facial images into numeric landmark representations. This approach reduces reliance on demographic visual cues such as ethnicity and race, while enabling an explainable analysis based on facial asymmetry. Specifically, MFM is used to detect the human face and extract facial landmark coordinates, which serve as the input for computing asymmetric facial numeric features. MFM is one of the MediaPipe framework libraries capable of determining 468 facial landmark coordinate points of human facial geometry (green dots in Figure 1). MFM is Google's pre-trained library which derives three-dimensional positioning from a two-dimensional image [11]. It combines a lightweight detector model called BlazeFace, which functions to crop the face from the original image for processing by a subsequent landmark generator model that predicts the facial surface and assigns precise positions to the landmarks [12]. In addition, MFM is optimized for extracting facial features efficiently in environments with limited hardware resources [13].

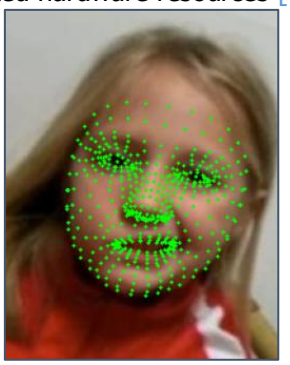

Figure 1. MediaPipe Face Mesh coordinate points

In contrast to prior studies that rely on deep learning architectures, this study proposes an explainable framework based on asymmetric facial numeric features extracted from static images. The proposed approach enables effective differentiation between Bell's palsy and stroke under limited data availability and hardware constraints, while also facilitating interpretable analysis of feature contributions relevant to facial asymmetry.

Methodology

The proposed method is structured into four major stages as presented in Figure 2. The first stage is feature engineering, which consists of facial feature extraction and dataset-based class assignment, where labels are determined according to the source of the images. The second stage is data preprocessing, which includes label encoding, class balancing through

undersampling, and data cleaning. The third stage consists of data splitting and SVM modeling. The fourth stage focuses on model evaluation.

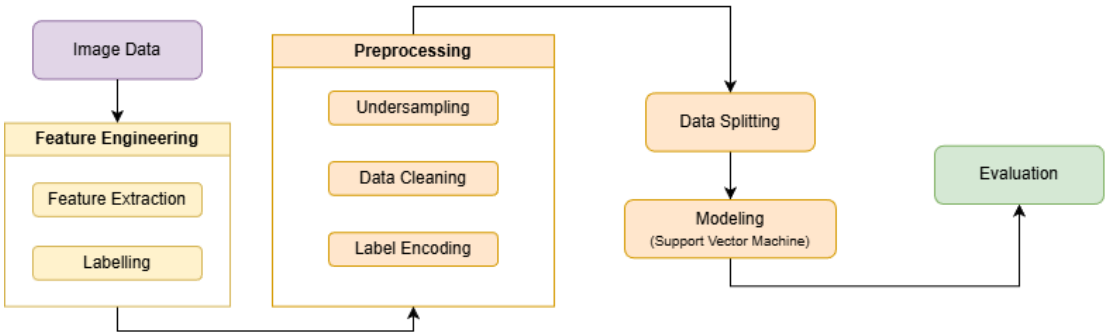

Figure 2. Proposed methodology flow

Dataset Description

The Bell's Palsy dataset was collected from HuggingFace [14], while the Stroke datasets were sourced from Kaggle [15], [16]. The first Kaggle dataset contains 1,029 stroke-labeled images, and the second contains 1,259 images, resulting in a total of 2,283 Stroke images. Meanwhile, the HuggingFace dataset contains 27 videos of bell's palsy patients. To address this limitation, each .mp4 video was converted into .jpg images using a frame-skipping strategy, producing approximately 400 images per video or all available frames if the total frame count was below 400. This process resulted in a total of 10,758 Bell's Palsy images.

Feature Engineering

The image data were converted into numerical features using MFM (see Figure 1). The coordinates of the eyebrows, eyes, nose, and both mouth corners are required to compute facial asymmetry. Therefore, all the coordinates mentioned were extracted along both the X and Y axes using MFM. The extracted coordinates for each class (BP and ST) were then saved into separate CSV files, with the column structure shown in Table 1. Labelling process conducted by adding one extra column in each CSV files. 'BP' for Bell's Palsy CSV and 'ST' for Stroke CSV. The labelling is source-based labelling because each dataset exclusively contained images from a single class. Finally, the labelled 'BP' and 'ST' CSV files were combined and saved into a single CSV file.

Table 1. Numerical features - the extracted coordinates

Index	Column Name
0	file
1	label
2	left_eyebrow_x
3	left_eyebrow_y
4	right_eyebrow_x
5	right_eyebrow_y
6	left_eye_x
7	left_eye_y
8	right_eye_x
9	right_eye_y
10	nose_x
11	nose_y
12	mouth_left_x
13	mouth_left_y
14	mouth_right_x
15	mouth_right_y

To compute the asymmetric facial features, Min-Max scaling, Euclidean distance, and angle calculation were performed. Min-Max scaling is used to normalize all landmark coordinates so that the features become relative to the face rather than global pixel values. Euclidean distance was used to measure the differences in distance between the left and right sides of the face. Finally, angle computation was applied to quantify the angular difference between the two mouth corners.

$$x_{new} = \frac{x_i - x_{min}}{x_{max} - x_{min}} \quad (1)$$

$$d_{ij} = \sqrt{(x_i - x_j)^2 + (y_i - y_j)^2} \quad (2)$$

$$\theta = \frac{180}{\pi} tan^{-1}\left(\frac{y_2 - y_1}{x_2 - x_1}\right) \quad (3)$$

Equation (1) shows the Min–Max scaling method used in this study. Equation (2) shows the Euclidean distance calculation, where (x1, y1) is the first coordinate and (x2, y2) is the second coordinate. Equation (3) shows the angle calculation method used in this study. After the computation, the asymmetric facial features were saved into a single CSV file, with the column structure shown in Table 2.

Table 2. Numerical features - asymmetric facial features

Index	Column Name
0	file
1	label
2	delta_eyebrow_y
3	delta_eyebrow_x
4	delta_eye_y
5	delta_eye_x
6	dist_eye_left_to_nose
7	dist_eye_right_to_nose
8	delta_eye_nose
9	dist_mouth
10	mouth_angle x

Preprocessing

The preprocessing of the asymmetric facial feature numerical data consists of three processes. First is the encoding of each label into binary form, where "ST" is encoded as 0 and "BP" as 1. Second is the examination of the number of entries for each label. The label with a greater number of entries is reduced so that it matches the number of entries of the label with fewer samples (undersampling). Third is the removal of the unused column, specifically the "file" column.

Data Splitting

After obtaining a balanced dataset with a 1:1 ratio between Bell's Palsy and Stroke through undersampling, the data were divided into training and testing sets using three splitting ratios (70:30, 80:20, and 90:10). The detailed class distribution for each ratio is presented in Table 3. These three ratios are used to ensure a more reliable evaluation, as relying on a single ratio may introduce bias and fail to represent the model's performance across different data distributions. Stratification was applied to ensure that the class distribution remained proportional in both the training and testing sets.

Table 3. Data splitting details

Ratio	Subset	BP	ST	Total
70:30	Train	1595	1595	3190
70:30	Test	684	684	1368
80:20	Train	1823	1823	3646
80:20	Test	456	456	912
90:10	Train	2051	2015	4102
90:10	Test	228	228	456

Modelling

This study employed Support Vector Machine (SVM) for classification. The extracted facial asymmetry features demonstrate nonlinear patterns, indicating that the classes cannot be separated using a linear hyperplane. Therefore, the Radial Basis Function (RBF) kernel was selected, as it is widely used for handling non-linear data distributions and has demonstrated strong classification performance across various domains [17], [18]. To ensure a fair and reproducible baseline evaluation, the default RBF hyperparameters (C = 1 and gamma = 'scale') were utilized. The objective of this study was to assess the discriminative capability of the proposed asymmetric facial features rather than to maximize classifier performance through extensive hyperparameter tuning. Therefore, systematic optimization procedures such as grid search were considered beyond the scope of the present work.

The Gaussian RBF kernel can be expressed using the following equation:

$$k(x_1 x_2) = \exp(-\gamma \|x_1 - x_2\|^2) \quad (4)$$

Information:

k : kernel
x_1, x_2 : input feature vectors
$\exp$: exponential function (ensures the kernel output is between 0 and 1)
γ : gamma

Evaluation

A confusion matrix was employed to analyze class-level prediction performance. The confusion matrix consists of True Positive (TP), False Positive (FP), True Negative (TN), and False Negative (FN), as presented in Table 4. Based on these values, the classification report metrics such as Accuracy, Precision, Recall, and F1-Score can be computed.

Table 4. Confusion matrix components

Component	Column Name
TP	The model correctly predicts Bell's Palsy.
FP	The model incorrectly predicts Bell's Palsy, but the actual label is Stroke.
TN	The model correctly predicts Stroke.
FN	The model incorrectly predicts Stroke, but the actual label is Bell's Palsy.

To further assess the robustness and generalization capability of the proposed SVM model, stratified 5-fold cross-validation was conducted. The training data were divided into five stratified folds, and the model was trained and validated iteratively across them. The average accuracy and standard deviation were reported to provide a more reliable estimate of model performance.

Furthermore, a learning curve analysis was performed to evaluate the model's behavior with respect to varying training set sizes. Learning curve shows the training and validation metric. This analysis helps identify potential overfitting or underfitting by comparing training and validation performance trends as the training size increases.

Results and Discussions

The feature engineering extracted the numerical data from image data using MFM which resulting in 10,754 entries of BP data and 2,279 entries of ST data. There were four images in each of the BP and ST folders where the face could not be detected by MFM, resulting in a total of eight undetected images, as shown in Figure 3.

Figure 3. Undetected facial images

After label encoding, undersampling was performed by reducing the number of BP entries to match the number of ST entries, resulting in 2,279 samples for each class. Next, the "file" column was removed before the data were split into the 70:30, 80:20, and 90:10 ratios as shown in Table 3. The SVM model was trained using the training set, and its performance was evaluated on the unseen testing set. The confusion matrix presented in Figure 4 summarizes the classification results obtained from the testing data, thereby reflecting the model's generalization performance on unseen samples. The ratio-specific results in Table 5 and Table 6 are also provided for further analysis.

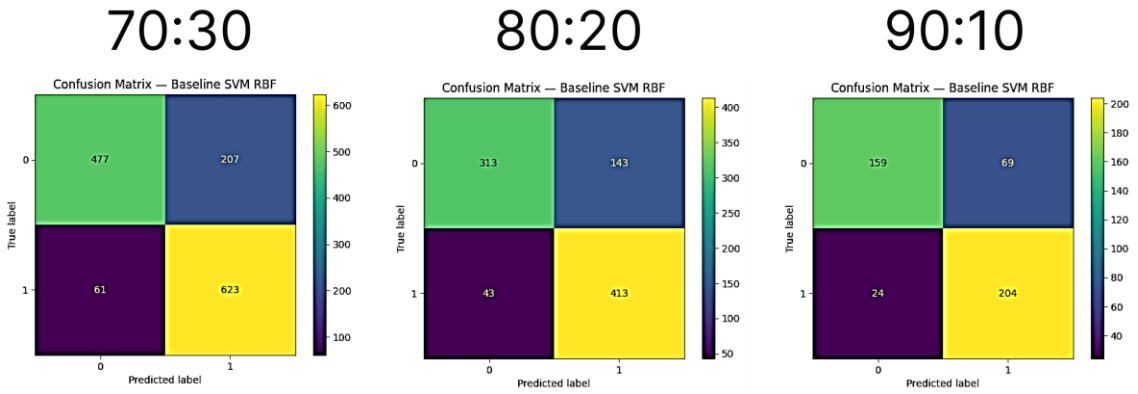

(a) (b) (c)

Figure 4. Confusion matrix for 70:30 ratio (a), 80:20 ratio (b), and 90:10 ratio (c)

Table 3. Classification report 70:30 ratio

	precision	recall	F1-score	support
0	0.89	0.70	0.78	684
1	0.75	0.91	0.82	684
Accuracy			0.80	1368
avg Macros	0.82	0.80	0.80	1368
Weighted avg	0.82	0.80	0.80	1368

Table 4. Classification report 80:20 ratio

	precision	recall	F1-score	support
0	0.88	0.69	0.77	456
1	0.74	0.91	0.82	456
Accuracy			0.80	912
avg Macros	0.81	0.80	0.79	912
Weighted avg	0.81	0.80	0.79	912

Table 5. Classification report 90:10 ratio

	precision	recall	F1-score	support
0	0.87	0.70	0.77	228
1	0.75	0.89	0.81	228
Accuracy			0.80	456
avg Macros	0.81	0.80	0.79	456
Weighted avg	0.81	0.80	0.79	456

The 70:30 ratio results show that the baseline model performs well in detecting the positive class as indicated by its high recall value. However, the lower precision suggests that the model still misclassifies some negative (Stroke) samples as positive (Bell's Palsy). This aligns with recent clinical findings showing that around 76% of acute ischemic stroke patients with central facial palsy exhibit upper facial weakness, including the eyebrows [19]. This overlap in asymmetric patterns between Bell's Palsy and certain Stroke cases may reduce class separability, contributing to false positive predictions and thereby affecting precision, while maintaining relatively high recall for detecting facial paralysis. As a result, facial asymmetry in Stroke is not limited to the lower face but also involves the eye and eyebrow regions, making it difficult to distinguish Stroke from Bell's Palsy using static facial images alone. The 80:20 baseline results indicate similar detection ability for the positive class, with the same recall value of 0.91. But its lower precision in positive class and lower recall in negative class makes it less favourable than the 70:30 baseline model. The 90:10 baseline results also show inferior performance compared to the 70:30 ratio, as its accuracy matches that of the 80:20 baseline model, and both its precision and recall are lower than the values obtained with the 80:20 ratio.

Within medical contexts, sensitivity (recall) is a critical metric, as its value can significantly affect treatment outcomes [20]. Based on this consideration, the 70:30 ratio provides the best performance, as it achieves the highest recall among the three ratios. The 80:20 and 90:10 ratios show lower recall values, making them less suitable for medical classification where missing positive cases must be minimized.

Although the confusion matrix provides detailed class-level performance on the testing set, it reflects only a single train–test partition. To ensure that the observed performance is not dependent on a particular data split and to further assess model stability, stratified 5-fold cross-validation was conducted on the training data for each ratio.

Table 6 presents the comparative performance of the proposed SVM model under three different data-splitting scenarios. The 70:30 configuration demonstrates the smallest generalization gap and the highest testing accuracy, indicating the most stable generalization performance. Although the 80:20 configuration yields a slightly higher mean accuracy, its larger standard deviation (0.0239) suggests greater performance fluctuation across folds. Furthermore, the testing accuracy of the 70:30 split is closely aligned with its cross-validation mean, indicating minimal generalization gap and reduced overfitting risk.

Table 6. Performance comparison across data splitting ratios

Split Ratio	CV Mean Accuracy	CV Std Dev	Test Accuracy	Generalization Gap
70:30	0.8072	0.0069	0.8041	0.0031
80:20	0.8110	0.02389	0.7961	0.0149
90:10	0.8084	0.0085	0.7961	0.0123

In addition to cross-validation, learning curve analysis was performed to examine the model's behavior as the number of training samples increased, as presented in Figure 5. For the 70:30 split, both training and validation accuracies increased gradually and converged with a consistently small gap, indicating stable learning and minimal overfitting. The 80:20 split achieved a slightly higher final validation accuracy; however, its training curve showed greater fluctuations, suggesting higher variance. Meanwhile, the 90:10 split exhibited less stable convergence at larger training sizes, with minor performance fluctuations toward the end. Overall, Figure 5 confirms that the 70:30 configuration provides the most stable and balanced generalization performance among the three ratios.

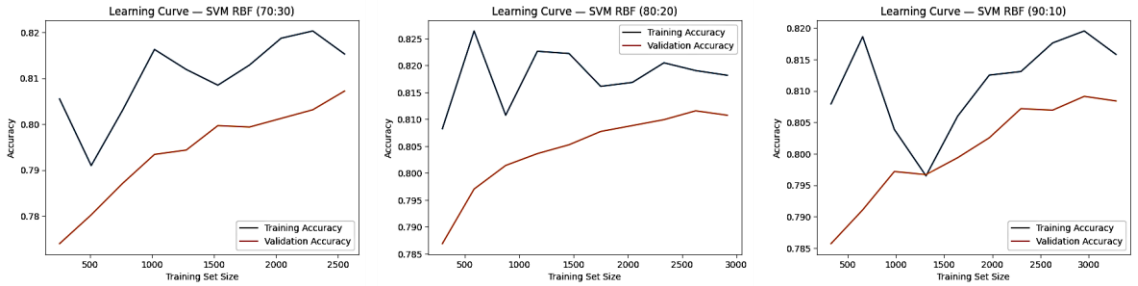

Figure 5 Learning Curve for 70:30 Ratio (a), 80:20 Ratio (b), and 90:10 Ratio (c)

The combined results from cross-validation and learning curve analysis indicate that the proposed SVM model does not exhibit significant overfitting or underfitting. For the 70:30 configuration, the mean cross-validation accuracy was 0.8072 with a low standard deviation of 0.0069, while the corresponding testing accuracy was 0.8041, resulting in a minimal generalization gap of approximately 0.0031. Similarly, the 80:20 and 90:10 splits produced cross-validation means of 0.8110 and 0.8084, with testing accuracies of 0.7961 for both configurations, yielding moderate gaps of 0.0149 and 0.0123, respectively. In the learning curve analysis, the gap between training and validation accuracies remained consistently small (approximately 0.01–0.02) across all splits, with validation performance stabilizing around 0.80–0.81. These findings demonstrate that the model achieves a balanced bias–variance trade-off and maintains stable generalization performance, particularly under the 70:30 configuration.

Conclusion

The proposed SVM-based framework successfully differentiates Bell's Palsy and Stroke using asymmetric facial numeric features extracted from static images, achieving stable generalization performance under limited data and computational constraints. This study proposed an explainable classification framework for differentiating Bell's Palsy (BP) and Stroke (ST) based on asymmetric facial numeric features extracted using MediaPipe Face Mesh. The extracted coordinates were transformed into numerical features through Min–Max scaling, Euclidean distance, and angle computation. The model avoids direct reliance on raw facial appearance while enabling interpretable feature representation.

To address class imbalance in the collected datasets, undersampling was applied to construct a balanced dataset. Among the three evaluated splitting ratios (70:30, 80:20, and

90:10), the 70:30 configuration demonstrated the most stable and reliable performance, achieving a testing accuracy of 0.8041 and a cross-validation mean accuracy of 0.8072 ± 0.0069, with a minimal generalization gap of approximately 0.0031. Learning curve analysis further confirmed stable convergence with a small training–validation gap (≈0.01–0.02), indicating a balanced bias–variance trade-off and minimal overfitting.

From a clinical perspective, the 70:30 configuration is preferable due to its higher recall, which is critical in medical screening scenarios where minimizing missed positive cases is essential. The 80:20 and 90:10 ratios yielded lower recall values, making them less suitable for this diagnostic task. Overall, the findings demonstrate that asymmetric facial geometric features combined with an SVM-RBF classifier can effectively distinguish Bell's Palsy from Stroke under limited dataset availability and hardware constraints. Rather than replacing deep learning approaches, this framework provides an interpretable and resource-efficient alternative suitable for environments where large-scale annotated datasets are unavailable.

Future research may focus on expanding available Bell's Palsy and Stroke datasets to improve data diversity and generalization performance. Incorporating temporal information from video-based facial sequences could enable analysis of dynamic muscle movements rather than relying solely on static images. Additionally, future studies may explore hybrid feature representations that combine geometric asymmetry features with other discriminative descriptors, conduct controlled comparisons with lightweight deep learning architectures, and evaluate alternative SVM kernel configurations to further optimize classification performance. Further analytical extensions, such as quantitative feature contribution analysis (e.g., correlation analysis or feature ranking), may also be performed to provide deeper insight into the relative importance of individual asymmetric features. Expanding the framework to include a healthy control class may also enable more comprehensive multi-class diagnostic modelling.

References

[1] S. J. Murphy and D. J. Werring, "Stroke: causes and clinical features," *Medicine*, vol. 48, no. 9, pp. 561–566, 2020, doi: 10.1016/j.mpmed.2020.06.002.

[2] S. Umirzakova, S. Ahmad, S. Mardieva, S. Muksimova, and T. K. Whangbo, "Deep learning-driven diagnosis: A multi-task approach for segmenting stroke and Bell's palsy," *Pattern Recognit.*, vol. 144, Dec. 2023, doi: 10.1016/j.patcog.2023.109866.

[3] J. Rajangam *et al.*, "Bell Palsy: Facts and Current Research Perspectives," *CNS Neurol. Disord. Drug Targets*, vol. 23, no. 2, pp. 203–214, Mar. 2023, doi: 10.2174/1871527322666230321120618.

[4] B. Boodale, M. Amin, K. Sabetian, D. Quesada, and T. Torrico, "Medial Pontomedullary Stroke Mimicking Severe Bell's Palsy: A Case Report," *Clin. Pract. Cases Emerg. Med.*, vol. 4, no. 3, pp. 380–383, Jul. 2020, doi: 10.5811/cpcem.2020.5.46965.

[5] M. Pohl *et al.*, "Ischemic stroke mimics: A comprehensive review," *Journal of Clinical Neuroscience*, vol. 93, pp. 174–182, Nov. 2021, doi: 10.1016/j.jocn.2021.09.025.

[6] P. N. A. Darmawan, N. M. D. Pratiwi, and I. K. Arimbawa, "Characteristic of Bell's Palsy in Clinical Neurologic at Sanglah Hospital Denpasar Bali Indonesia," *International Journal of Research and Review*, vol. 8, no. 12, pp. 318–322, Dec. 2021, doi: 10.52403/ijrr.20211239.

[7] S. Gupta, M. K. Jawanda, N. Taneja, and T. Taneja, "A systematic review of Bell's Palsy as the only major neurological manifestation in COVID-19 patients," *Journal of Clinical Neuroscience*, vol. 90, pp. 284–292, Aug. 2021, doi: 10.1016/j.jocn.2021.06.016.

[8] Y. I. Royan, P. Pramono, and A. A. K. Asri, "Performance Comparison of Convolutional Neural Networks (CNN) and Support Vector Machine (SVM) Algorithms in Human Face Classification," *G-Tech: Jurnal Teknologi Terapan*, vol. 9, no. 3, pp. 1544–1553, Jul. 2025, doi: 10.70609/g-tech.v9i3.7384.

[9] F. Mahardhika, M. L. Haryanti, and P. Hiskiawan, "Performance Evaluation of Speech Emotion Recognition Using Hybrid Feature Selection and Machine Learning," in *2025 4th International Conference on Creative Communication and Innovative Technology (ICCIT)*, Kota Cirebon, Indonesia: IEEE, Sep. 2025, pp. 1–7. doi: 10.1109/ICCIT65724.2025.11166879.

[10] Lukman Arif Sanjani, R. Bimo Mandala Putra, and U. Laili Yuhana, "Exploring the Application of Machine Learning for Automatic Inbound Email Classification in CRM System at XYZ Company," *Journal of Technology and Informatics (JoTI)*, vol. 6, no. 1, pp. 1–7, Oct. 2024, doi: 10.37802/joti.v6i1.715.
[11] S. Baul, Md. Ratan Rana, N. Jahan Trisna, and F. Bente Alam, "Development of a Real-time Driver's Drowsiness Detection System Using MediaPipe Face Mesh," *International Journal of Engineering and Manufacturing*, vol. 15, no. 5, pp. 46–57, Oct. 2025, doi: 10.5815/ijem.2025.05.04.
[12] J. Jose, K. Raimond, and S. Vincent, "SleepyWheels: An Ensemble Model for Drowsiness Detection leading to Accident Prevention," Nov. 2022. doi: 10.48550/arXiv.2211.00718.
[13] D. Ciraolo, M. Fazio, R. S. Calabrò, M. Villari, and A. Celesti, "Facial expression recognition based on emotional artificial intelligence for tele-rehabilitation," *Biomed. Signal Process. Control*, vol. 92, Jun. 2024, doi: 10.1016/j.bspc.2024.106096.
[14] Jasir, "jasir/palsynet-data." Accessed: Dec. 06, 2025. [Online]. Available: https://huggingface.co/datasets/jasir/palsynet-data
[15] M. Kaitav, "Facial_Droop_and_Facial_Paralysis_image." Accessed: Dec. 06, 2025. [Online]. Available: https://www.kaggle.com/datasets/kaitavmehta/facial-droop-and-facial-paralysis-image
[16] J. Danish, "Face Images of Acute Stroke and Non Acute Stroke." Accessed: Dec. 06, 2025. [Online]. Available: https://www.kaggle.com/datasets/danish003/face-images-of-acute-stroke-and-non-acute-stroke
[17] M. Alfonso and D. Bhisetya Rarasati, "JISA (Jurnal Informatika dan Sains) Sentiment Analysis of 2024 Presidential Candidates Election Using SVM Algorithm," *JISA (Jurnal Informatika dan Sains)*, vol. 6, no. 2, pp. 110–5, Dec. 2023, doi: doi.org/10.31326/jisa.v6i2.1714.
[18] F. Tampinongkol, "Identifikasi Penyakit Daun Tomat Menggunakan Gray Level Co-occurrence Matrix (GLCM) dan Support Vector Machine (SVM)," *Techno Xplore : Jurnal Ilmu Komputer dan Teknologi Informasi*, vol. 8, no. 1, pp. 08–16, Apr. 2023, doi: 10.36805/technoxplore.v8i1.3578.
[19] N. Fariesya Suhaila Md Sazihan, N. Mu, azzah Abdul Latiff, N. Noordini Nik Abd Malik, S. Mashohor, and F. Taha Al-Dhief, "Evaluating the Effectiveness of Parameter Tuning for Support Vector Machine on Voice Pathology Database," *Elektrika*, vol. 24, no. 2, pp. 118–124, 2025, doi: 10.11113/elektrika.v24n2.628.
[20] D. Asmawati, L. Arif Sanjani, C. Dimas Renggana, C. Fatichah, and T. Mustaqim, "Arrhythmia Classification with ECG Signal using Extreme Gradient Boosting (XGBoost) Algorithm," *Journal of Technology and Informatics (JoTI)*, vol. 6, no. 1, pp. 36–42, Oct. 2024, doi: 10.37802/joti.v6i1.792.